

## Self-consistent electronic structure of 3d-transition-metal impurities in aluminum using the recursion method

Prabhakar P. Singh

*Department of Materials Science and Mineral Engineering, University of California, Berkeley, California 94720*

(Received 1 March 1990; revised manuscript received 13 August 1990)

For developing an accurate first-principles technique for describing the electronic structure of systems without perfect periodicity, we have performed self-consistent electronic-structure calculations for dilute alloys of 3d-transition-metal impurities in aluminum using the recursion method with the tight-binding linear muffin-tin orbitals (TB-LMTO) Hamiltonian. Using the self-consistent potential at the impurity site, we investigate the changes in the local density of states and the charge transfer between the impurity and the neighboring host atoms. The results are in good agreement with the more accurate Green's-function-LMTO [Phys. Rev. B **33**, 5307 (1986)] results, thereby confirming the accuracy of the present approach.

### I. INTRODUCTION

The need for an accurate and reliable method for describing the electronic structure of systems without perfect translational symmetry has become of paramount importance due to recent developments in solid-state technology where the effects of surfaces, defects, and impurities can no longer be ignored. In many cases, a local description rather than a "Bloch-like" description of the electronic structure is more appropriate and at times it is the only possible description. Very often periodicity is restored by using the supercell methods. One of the disadvantages of the supercell method is that it may result in artificial interference between the different supercells, thereby distorting the description of the real system.

With the aim of developing a reliable and accurate first-principles technique for describing the electronic structure based on a local description, we have used the tight-binding linear muffin-tin orbital (TB-LMTO) Hamiltonian<sup>1-3</sup> in the recursion method<sup>4</sup> to study, self-consistently, 3d-transition-metal impurities in aluminum. The use of the TB-LMTO Hamiltonian affords a direct comparison of the recursion results with the results of the more accurate Green's-function-LMTO method,<sup>5,6</sup> leading to a better understanding of the limitations and the approximations of the present approach.

The problem of impurities in metals has now been studied for more than 35 years. Since Friedel's explanation of the changes in the transport properties of alloys using the virtual-bound-state model<sup>7,8</sup> there have been a number of other models for describing the electronic structure of alloys. The approaches which have been followed include the Anderson impurity model,<sup>9</sup> the localized interaction of Wolff,<sup>10</sup> and the localized spin-fluctuation model.<sup>11</sup>

The introduction of an impurity atom can change the

host lattice by perturbing the electronic charge distribution as well as the positions of the neighboring host atoms. To simplify the problem we assume that at the neighboring host atoms the potentials as well as the positions are not perturbed. The perturbation of neighboring atom potentials can be taken into account but it requires a substantial computational effort. The effect of lattice relaxation can be incorporated by defining a new effective nuclear charge<sup>12</sup> but we do not follow this procedure. Starting with these approximations we express the full Hamiltonian of the perturbed crystal in terms of the TB-LMTO Hamiltonian and then a self-consistent calculation of the electronic structure of the impurity in a cluster is carried out using the recursion method. We call this approach the Green's-function recursion method and use it to study, self-consistently, the electronic structure of 3d-transition-metal impurities in aluminum. Our results are in agreement with the results of the Green's-function-LMTO method<sup>6,13</sup> as well as with the calculations of Deutz, Dederichs, and Zeller.<sup>14</sup>

The paper is organized as follows: In Sec. II we describe the self-consistent Green's-function recursion method using the TB-LMTO approach. The approximations due to the recursion and due to the use of an approximate Hamiltonian are discussed in Sec. III. Section IV contains the results for 3d impurities in aluminum. Finally, ways to improve our results are indicated in Sec. V.

### II. RECURSION IN THE TB-LMTO METHOD

The solution of the alloy problem is essentially a two-step process. First we solve the problem of the perfect crystal and obtain the electronic structure of the host solid. Then we replace one of the host atoms by an impurity and try to obtain the electronic structure of the perturbed crystal or alloy. We can express the solution,

at least formally, in terms of the Green's function of the perturbed crystal. An approach based on solving directly for the Green's function of the perturbed crystal can be developed using the recursion method.

### A. Electronic structure of the host solid

A number of methods can be used for describing the electronic structure of the host solid. Some of the methods in use are the (i) linear combination of atomic orbitals, (ii) orthogonalized-plane-wave method,<sup>15</sup> (iii) pseudopotential method,<sup>16</sup> (iv) Korringa-Kohn-Rostoker method,<sup>17</sup> (v) augmented-plane-wave method,<sup>18</sup> (vi) linear augmented-plane-wave method,<sup>19</sup> and (vii) LMTO method.<sup>19,20</sup>

The LMTO method of Andersen has been successfully applied to describe the electronic structure of elemental metals,<sup>20</sup> metallic compounds,<sup>21</sup> molecules,<sup>22</sup> microclusters,<sup>23</sup> amorphous materials,<sup>24,25</sup> and others. The relative ease and efficiency in implementing the LMTO method, coupled with the physical transparency with which it describes the electronic structure, make it very useful. The method has been described in many papers and reviews by Andersen and co-workers.<sup>2,3,19,20</sup>

A unique advantage of using the LMTO method is the exact transformation of the long-ranged LMTO Hamiltonian into a first-principles tight-binding Hamiltonian, which can then be used to investigate the local properties of systems without perfect translational symmetry. The LMTO approach can also be used to compare the accuracy of  $\mathbf{k}$ -space methods with that of  $\mathbf{R}$ -space methods. We use the LMTO method for calculating the self-consistent electronic structure of the host solid, aluminum, and the TB-LMTO method for describing the impurity in a cluster. In the following we closely follow the notation of Ref. 2.

### B. Hamiltonian and overlap matrices

In order to use the recursion formalism, we have to specify the tight-binding Hamiltonian  $\mathbf{H}$  and the appropriate basis functions. We choose to work in the nearly orthogonal representation of the LMTO method, denoted by the superscript  $\gamma$ , in which the Hamiltonian and overlap matrices are<sup>1-3</sup>

$$\mathbf{H}^\gamma = \mathbf{E}_v + \mathbf{h}^\gamma + \mathbf{h}^\gamma \mathbf{E}_v \mathbf{p}^\gamma \mathbf{h}^\gamma \quad (1a)$$

and

$$\mathbf{O}^\gamma = \mathbf{I} + \mathbf{h}^\gamma \mathbf{p}^\gamma \mathbf{h}^\gamma, \quad (1b)$$

where

$$\mathbf{h}^\gamma = \mathbf{h}(\mathbf{I} + \mathbf{o}\mathbf{h})^{-1}. \quad (2)$$

The matrix elements of  $\mathbf{h}$  and the potential parameters  $\mathbf{E}_v$ ,  $\mathbf{o}$ , and  $\mathbf{p}^\gamma$  are defined in Refs. 2 and 6, and  $\mathbf{I}$  is the identity matrix. The nearly orthogonal orbitals are partially localized and the Hamiltonian decays exponentially in  $\mathbf{R}$  space.<sup>1-3</sup> We require a very localized Hamiltonian for keeping the calculation of the recursion coefficients to a manageable size. It is known that further localization of the interaction leads to nonorthogonal orbitals. Thus,

we have to calculate  $(\mathbf{O}^\gamma)^{-1/2} \mathbf{H}^\gamma (\mathbf{O}^\gamma)^{-1/2}$  and use this as the Hamiltonian. In order to do this, we first evaluate the Löwdin orthonormalized Hamiltonian<sup>26</sup>

$$\begin{aligned} (\mathbf{O}^\gamma)^{-1/2} \mathbf{H}^\gamma (\mathbf{O}^\gamma)^{-1/2} &= (\mathbf{I} - \mathbf{h}^\gamma \mathbf{p}^\gamma \mathbf{h}^\gamma / 2) \\ &\quad \times (\mathbf{E}_v + \mathbf{h}^\gamma + \mathbf{h}^\gamma \mathbf{E}_v \mathbf{p}^\gamma \mathbf{h}^\gamma) \\ &\quad \times (\mathbf{I} - \mathbf{h}^\gamma \mathbf{p}^\gamma \mathbf{h}^\gamma / 2) \\ &\approx \mathbf{E}_v + \mathbf{h}^\gamma, \end{aligned} \quad (3)$$

where we have ignored the potential parameter  $\mathbf{p}^\gamma$ , which is generally small. We define Eq. (3) as the second-order Hamiltonian  $\mathbf{H}^{(2)}$ , i.e.,

$$\mathbf{H}^{(2)} = \mathbf{E}_v + \mathbf{h}^\gamma. \quad (4)$$

The Hamiltonian  $\mathbf{H}^{(2)}$  is correct up to second order in  $(E - E_v)$  and it decays exponentially in  $\mathbf{R}$  space due to the exponential decay of  $\mathbf{S}^\gamma$ .<sup>1-3</sup> It can be used as the Hamiltonian if we desire the accuracy that it offers and are willing to increase the size of the cluster for calculating the recursion coefficients because of the long range of the interaction. A simpler and more efficient approach is to express  $\mathbf{S}^\gamma$  in terms of the most localized structure matrix  $\mathbf{S}^\beta$ , i.e.,

$$\mathbf{S}^\beta = \mathbf{S}^\gamma [1 + (\gamma - \beta) \mathbf{S}^\gamma]^{-1}. \quad (5)$$

The potential parameters  $\gamma_l$  and the tight-binding parameters  $\beta_l$  are defined in Refs. 2 and 6. The superscript  $\beta$  denotes the tight-binding representation of the LMTO method. Now  $\mathbf{h}^\gamma$ , Eq. (2), can be written as

$$\mathbf{h}^\gamma = \mathbf{h}^\beta (\mathbf{I} + \mathbf{o}^\beta \mathbf{h}^\beta)^{-1}. \quad (6)$$

Then substituting for  $\mathbf{h}^\gamma$  from Eq. (6) in Eq. (4), we get

$$\begin{aligned} \mathbf{H}^{(2)} &= \mathbf{E}_v + \mathbf{h}^\beta (\mathbf{I} + \mathbf{o}^\beta \mathbf{h}^\beta)^{-1} \\ &= \mathbf{E}_v + \mathbf{h}^\beta - \mathbf{h}^\beta \mathbf{o}^\beta \mathbf{h}^\beta + \mathbf{h}^\beta \mathbf{o}^\beta \mathbf{h}^\beta \mathbf{o}^\beta \mathbf{h}^\beta - \dots \\ &\approx \mathbf{E}_v + \mathbf{h}^\beta - \mathbf{h}^\beta \mathbf{o}^\beta \mathbf{h}^\beta \end{aligned} \quad (7a)$$

and

$$\mathbf{H}^{(1)} = \mathbf{E}_v + \mathbf{h}^\beta, \quad (7b)$$

where we have defined  $\mathbf{H}^{(1)}$  as the first-order Hamiltonian, as it is correct up to first order in  $(E - E_v)$ . The first-order Hamiltonian  $\mathbf{H}^{(1)}$  decays more rapidly than the second-order Hamiltonian  $\mathbf{H}^{(2)}$  because  $\mathbf{H}^{(1)}$  contains  $\mathbf{S}^\beta$  instead of  $\mathbf{S}^\gamma$ . Typically,  $\mathbf{H}^{(2)}$  vanishes after third- or fourth-nearest neighbors, while  $\mathbf{H}^{(1)}$  vanishes only after second-nearest neighbors for close-packed solids.<sup>1-3,6</sup> We use the first-order Hamiltonian  $\mathbf{H}^{(1)}$  for describing the interaction between the atoms in a cluster for calculating the recursion coefficients.

### C. Local density of states and charge density

For obtaining a self-consistent solution we need the electronic charge density inside the perturbed Wigner-Seitz (WS) sphere. Formally the charge density  $\rho(\mathbf{r})$  can be expressed in terms of the wave functions  $\psi^j(\mathbf{r})$  of the system, where  $j$  is the band index. The wave functions

can be constructed as

$$\psi^j(\mathbf{r}) = \sum_L \psi_L^j(\mathbf{r}) . \quad (8)$$

In Eq. (8) we have defined

$$\psi_L^j(\mathbf{r}) = \sum_{\mathbf{R}} a_L^j \chi_L(\mathbf{r} - \mathbf{R}) , \quad (9)$$

where  $a_L^j$  are the expansion coefficients,  $L \equiv (l, m)$  is the orbital index,  $\mathbf{R}$  denotes the atomic sites, and  $\chi_L(\mathbf{r})$  are the basis functions. Then the charge density is

$$\rho(\mathbf{r}) = \sum_j^{\text{occ}} \psi^{j*}(\mathbf{r}) \psi^j(\mathbf{r}) , \quad (10)$$

where the summation is over occupied states only. The evaluation of the charge density using Eq. (10) is evident-

ly laborious if the basis functions are not very localized. We also have to determine the expansion coefficients  $a_L^j$ .

A simpler approach for evaluating the spherically symmetric valence charge density,  $\rho(r)$ , inside the impurity cell is to use the local density of states and the partial wave solutions of the impurity potential, i.e.,

$$4\pi\rho(r) = \sum_l \int_{-\infty}^{E_F} 2n_l(E) \phi_l^2(E, r) dE , \quad (11)$$

where  $n_l(E)$  are the local density of states,  $\phi_l(E, r)$  are the partial wave solutions, and  $E_F$  is the Fermi energy. The factor of 2 takes care of the spin degeneracy. The partial waves  $\phi_l(E, r)$  are approximated by a Taylor-series expansion around some reference energy  $E_{vl}$ . Keeping terms up to  $(E - E_{vl})^2$  the expression for the electronic charge density becomes<sup>2,20</sup>

$$4\pi\rho(r) = \sum_l \left[ \phi_{vl}^2(r) N_l + 2\phi_{vl}(r) \dot{\phi}_{vl}(r) \int_{-\infty}^{E_F} 2n_l(E) (E - E_{vl}) dE \right] + \sum_l \left[ \dot{\phi}_{vl}^2(r) + \ddot{\phi}_{vl}(r) \phi_{vl}(r) \int_{-\infty}^{E_F} 2n_l(E) (E - E_{vl})^2 dE \right] + \dots , \quad (12)$$

where

$$N_l \equiv \int_{-\infty}^{E_F} 2n_l(E) dE \quad (13)$$

are the integrated local density of states and the overdots indicate the derivatives with respect to energy  $E$ . The local density of states

$$n_l(E) = -\frac{1}{\pi} \text{Im} G_{ll}(E) , \quad (14)$$

where  $G_{ll}(E)$  are the diagonal elements of the Green's function at the impurity site, is evaluated using the recursion method. The angular momentum  $l$  denotes  $s, p, e_g,$  and  $t_{2g}$  states. For terminating the recursion coefficients we use the Beer and Pettifor approach.<sup>27</sup> Once we have evaluated  $n_l(E)$  the charge density inside the impurity atom can be evaluated using Eq. (12).

#### D. Self-consistent impurity in a cluster problem

The Green's-function recursion method can be used to describe the electronic structure of impurities in crystal-line clusters. We assume that the impurity potential is localized within the impurity WS sphere. We also assume that the electronic density of states of the nearest neighbors remains unchanged. Under these assumptions the self-consistent calculation of the impurity potential reduces to a self-consistent calculation inside the impurity atom at the central site of the cluster. The effective one-electron potential,  $V(r)$ , inside the WS sphere is given by

$$V(r) = \int \frac{2\rho_{\text{tot}}(r')}{|r - r'|} dr' - \frac{2Z}{r} + V_{\text{xc}}(r) + V_M(r) , \quad (15)$$

where all the quantities refer to the impurity atom and  $\rho_{\text{tot}}(r)$  is the sum of valence and core charge densities. In Eq. (15),  $Z$  and  $V_{\text{xc}}(r)$  denote the nuclear charge and the exchange-correlation potential, respectively. The Madlung potential  $V_M(r)$  is not taken into account because we do not perturb the electronic density at the neighboring sites. The procedure followed for obtaining the self-consistent impurity electronic structure is outlined below.

(i) Construct the potential  $V(r)$  by renormalizing the free-atom electron density to the WS sphere.

(ii) Calculate the recursion coefficients and determine the local density of states for all symmetry-projected states given by Eq. (14).

(iii) Get the new electron density using Eq. (12) and the frozen core charge density.

(iv) Construct the new effective one-electron potential by solving Poisson's equation for the electron density and then adding  $-2Z/r$  and  $V_{\text{xc}}(r)$ .

(v) Solve the Schrödinger equation as described in Refs. 18 and 20.

Now the output potential obtained from (v) is used to set up the new impurity Hamiltonian and (ii)-(v) are repeated until self-consistency is achieved.

### III. APPROXIMATIONS IN THE GREEN'S-FUNCTION RECURSION METHOD

In the Green's-function recursion calculation the approximations are twofold: (i) those intrinsic to the recursion method and (ii) those related to the tight-binding Hamiltonian. A detailed description of the approximations involving (i) is given in Ref. 4. The approximations intrinsic to the LMTO Hamiltonian are discussed in

Refs. 1–3. We briefly outline the more important approximations of (i) and (ii) and suggest ways to correct for them.

#### A. Recursion method approximations

The most important approximation is due to the finite size of the cluster. The size of the cluster limits the number of recursion coefficients that can be calculated exactly, thereby limiting the accuracy of the local density of states. In most cases, it is possible to make a compromise between the cluster size and the desired accuracy in the local density of states. There are several ways by which the recursion coefficients in the tail can be approximated.<sup>4,28</sup>

#### B. Hamiltonian-related approximations

We use an approximate tight-binding Hamiltonian  $\mathbf{H}^{(1)}$ , which is correct up to first order in  $\mathbf{h}$ . For wide bands one should include the second-order term as well. Given the first-order Hamiltonian, we can get more accurate results by dividing the band in different energy panels by appropriately choosing different  $E_v$ 's. To improve upon the results obtained using the first-order Hamiltonian  $\mathbf{H}^{(1)}$ , we can use the second-order Hamiltonian  $\mathbf{H}^{(2)}$ , which requires an increase in the cluster size for calculating the same number of exact recursion coefficients.

### IV. RESULTS AND DISCUSSION

The electronic structure of  $3d$  impurities in Al is calculated using the Green's-function recursion method. The impurity atom is placed at the center of a 489-atom face-centered-cubic (fcc) cluster. The cluster is constructed so that five levels of recursion coefficients can be calculated exactly when we include up to second-nearest-neighbor interactions. The description of the host lattice, in this case that of Al, was calculated by the LMTO method.

The atomic wave functions of the impurity and host atoms are calculated by solving, self-consistently, the fully relativistic Dirac equation with free-atom boundary conditions. The electronic configurations and term values of atoms belonging to  $3d$  series of the Periodic Table are listed in Table I. During the self-consistent

TABLE I. Electronic configurations and term values for  $3d$  elements of the Periodic Table.

Element	Z	Electronic configuration	Term value
Ti	4	[Ar] $3d^24s^2$	$^3F_2$
V	5	[Ar] $3d^34s^2$	$^4F_{3/2}$
Cr	6	[Ar] $3d^54s^1$	$^7S_3$
Mn	7	[Ar] $3d^54s^2$	$^6S_{5/2}$
Fe	8	[Ar] $3d^64s^2$	$^5D_4$
Co	9	[Ar] $3d^74s^2$	$^4F_{9/2}$
Ni	10	[Ar] $3d^84s^2$	$^3F_4$
Cu	11	[Ar] $3d^{10}4s^1$	$^2S_{1/2}$

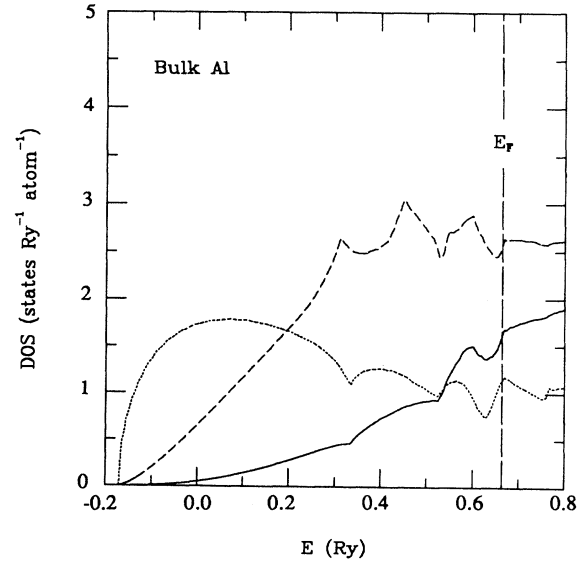


FIG. 1. The  $l$ -projected density of states for fcc Al using the LMTO method, including the combined correction terms. The dotted, dashed, and solid lines are  $s$ ,  $p$ , and  $d$  densities of states, respectively.

Green's-function recursion calculations we freeze the potential due to all core electrons. The exchange and correlation effects are included through the parametrization given by von Barth and Hedin.<sup>29</sup>

#### A. Electronic structure of bulk aluminum

The self-consistent electronic structure of Al is calculated with the LMTO method in the atomic-sphere approximation.<sup>2,3,19,20</sup> To account for some of the approxi-

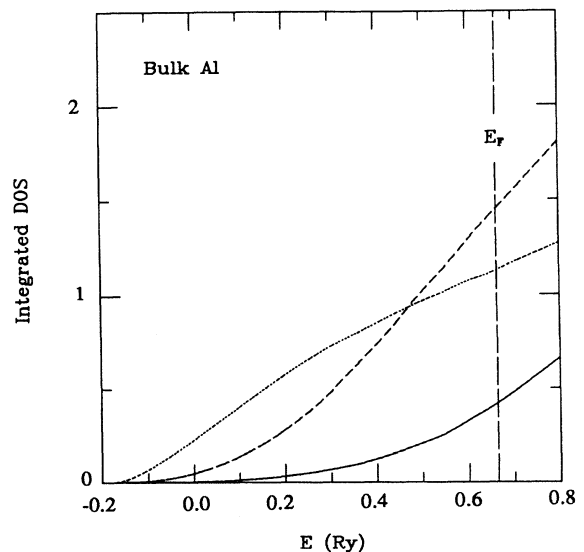


FIG. 2. The integrated density of states for fcc Al using the LMTO method, including the combined correction terms. The dotted, dashed, and solid lines are  $s$ ,  $p$ , and  $d$  integrated densities of states, respectively.

TABLE II. Summary of results for Al at the WS radius  $S=2.9778$  a.u.

Fermi energy (Ry)	-0.053
$V_{\text{MTZ}}$ (Ry)	-0.716
Number of $s$ electrons	1.130
Number of $p$ electrons	1.451
Number of $d$ electrons	0.419
DOS at $E_F$ (states/Ry)	5.309

mations resulting from the atomic-sphere approximation, we include the combined correction terms.<sup>19,20</sup> Our final self-consistent results do not depend on canonical scaling.<sup>20</sup> The Brillouin-zone integration was carried out with 916 points in an irreducible wedge of the Brillouin zone. The reference energy  $E_{vl}$  was chosen to be the center of gravity of the occupied part of the  $l$  band. The  $l$ -projected densities of states obtained from the self-

consistent potential parameters are shown in Fig. 1.<sup>6</sup> The density of states compares very well with the results in Refs. 30 and 31. Our calculated total density of states at the Fermi energy for the bulk Al is 5.309 states/Ry which is in good agreement with the results of Refs. 30 and 31 which are 5.578 and 5.46 states/Ry, respectively. The integrated densities of states are shown in Fig. 2. Our integrated  $s$ ,  $p$ , and  $d$  densities of states compare well with the results in Ref. 31, which are 1.55, 1.38, and 0.07, respectively. A summary of results for bulk Al is given in Table II.

### B. Electronic structure of 3d impurities in aluminum

A detailed account of all the results for the 3d impurities in Al is presented in this section. The results have been collected under the following categories: (i) local

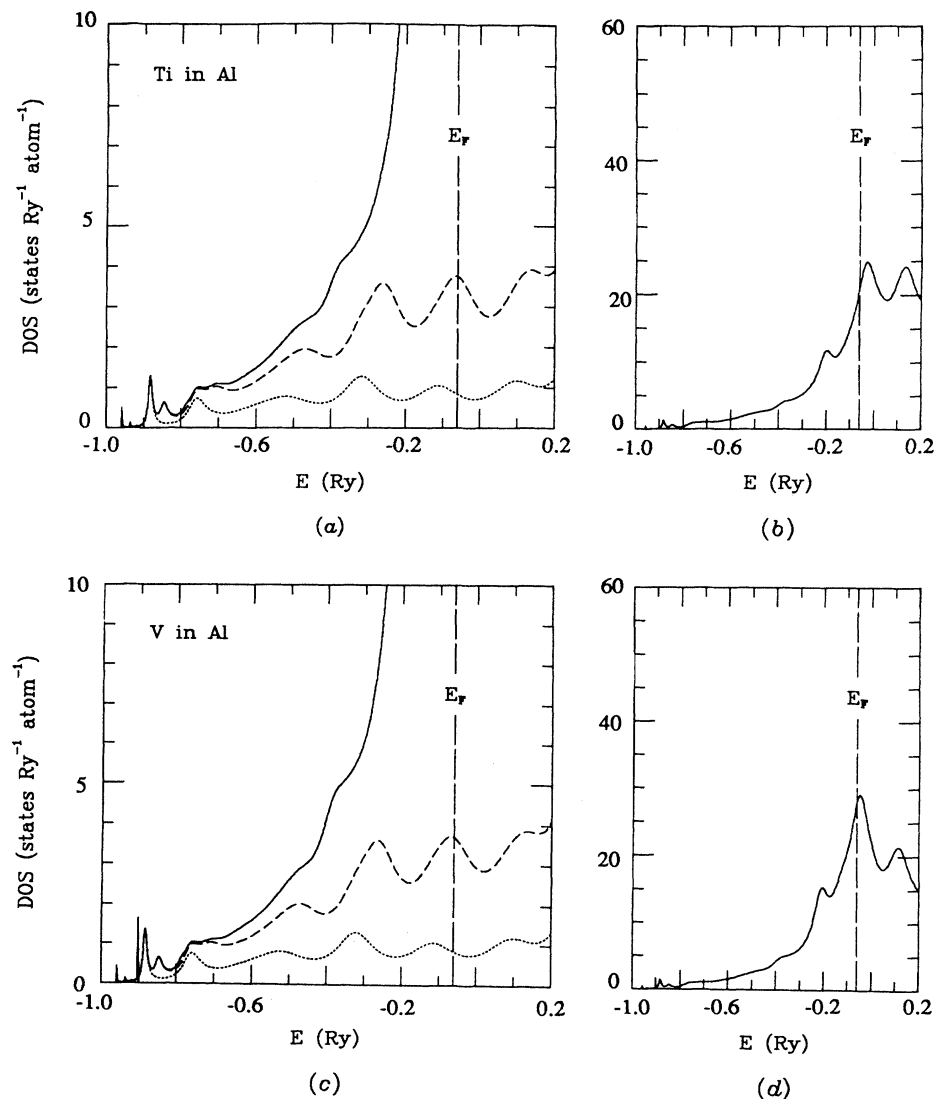


FIG. 3. DOS for Ti in Al (a) and (b) and V in Al (c) and (d) using the Green's-function recursion method. The dotted, dashed, and solid lines are  $s$ ,  $s+p$ , and  $s+p+d$  local densities of states, respectively.

density of states, (ii) charge transfer and screening, and (iii) virtual bound states

### 1. Local density of states

The changes in the energy spectrum of the perfect solid brought about by the impurity atom are clearly manifested in the local density of states at the impurity site as well as at the sites surrounding the impurity. In the case of dilute alloys, it is reasonable to assume that the changes in the local density of states will get smaller further away from the impurity site. Although it can be shown that the charge perturbation of the host atoms due to the impurity is long-ranged and oscillatory in nature, it is evident that the most dominant change in the density of

states occurs at the impurity site. The change at the impurity site is followed by smaller changes in atoms surrounding the impurity.

As a first approximation, we can assume that the changes in the density of states are localized at the impurity site and the host atoms surrounding the impurity retain their bulk density of states, i.e., they are bulklike. In metals the impurity is quickly screened, thereby localizing the perturbation. For the most part, the single-site approximation predicts results that are in good agreement with experiments. But in order to predict the charge transfer between impurity and host atoms more accurately, one should at least include the perturbation of the neighboring host atoms. The inclusion of nearest-neighbor perturbation becomes necessary because even a

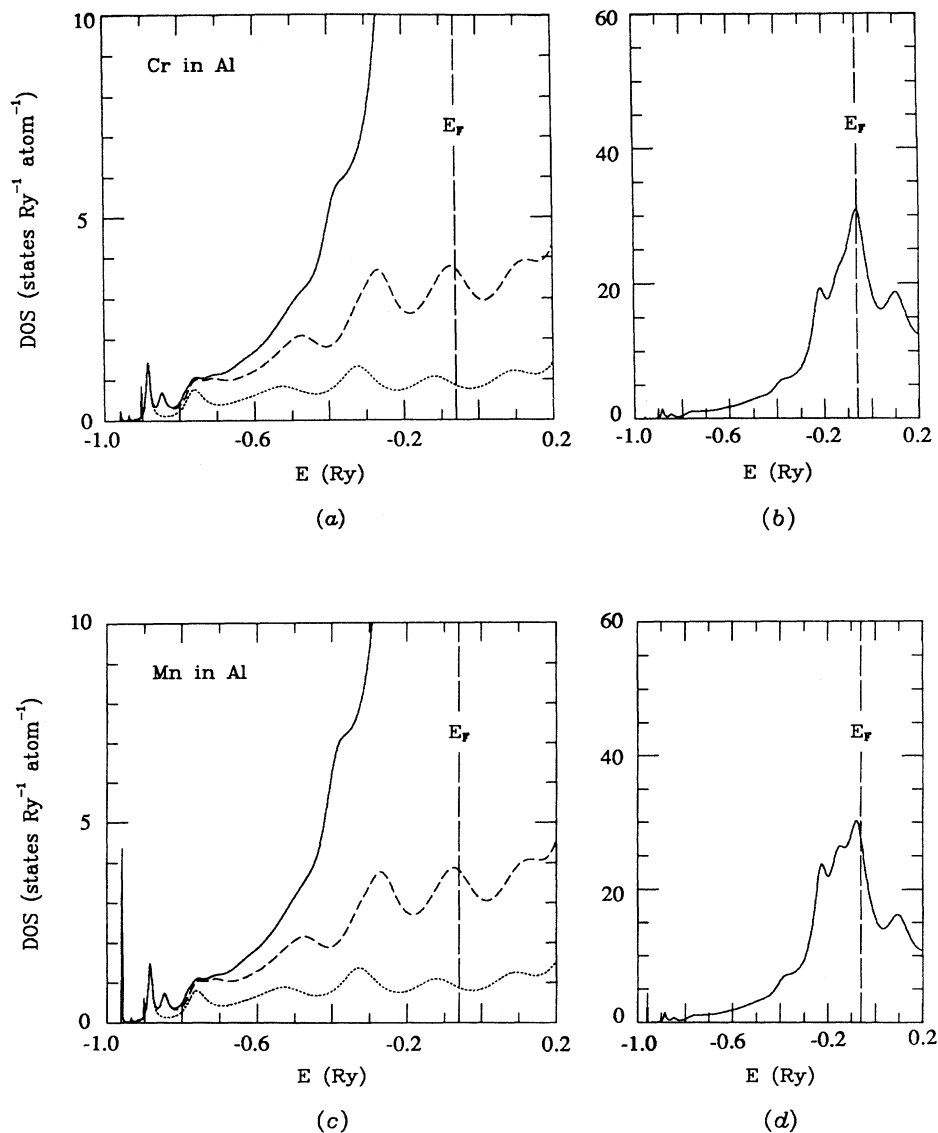


FIG. 4. DOS for Cr in Al (a) and (b) and Mn in Al (c) and (d) using the Green's-function recursion method. The key is as in Fig. 3.

small shift in the potential of the nearest-neighbor host atoms can lead to a rather large charge redistribution. That, in turn, will affect the local density of states at the impurity site. The computational effort involved in including the perturbation at the nearest-neighbor sites is prohibitive and we do not follow this procedure.

The self-consistent local densities of states (LDOS), for  $3d$  impurities in Al, calculated with the Green's-function recursion method are shown in Figs. 3–6. In these figures we show  $s$  (dotted line),  $s+p$  (dashed line), and  $s+p+d$  (solid line) densities of states, respectively. These LDOS can be easily understood in terms of the bulk density of states and the idea of resonance and antiresonance points. We see that the  $s$  and  $p$  densities of states do not change by much as we go through  $AlTi$  to

$AlCu$ . The large change in the  $d$  density of states represents the virtual bound states. The movement of the virtual bound state from well above the Fermi energy for  $AlTi$  to well inside for  $AlCu$  can be seen clearly.

The local densities of states at  $E_F$  at the impurity site are given in Table III. We also list the results of a separate Green's-function–LMTO calculations for  $3d$  impurities in Al.<sup>6</sup> In our Green's-function–LMTO calculations we express the Green's function at the impurity site in terms of the Green's function of the host lattice and the perturbing potential. With the assumption of only one perturbed muffin tin, as in the Green's-function recursion method, the resulting Dyson equation is solved self-consistently. Thus the differences between the two methods (Green's-function recursion and Green's-

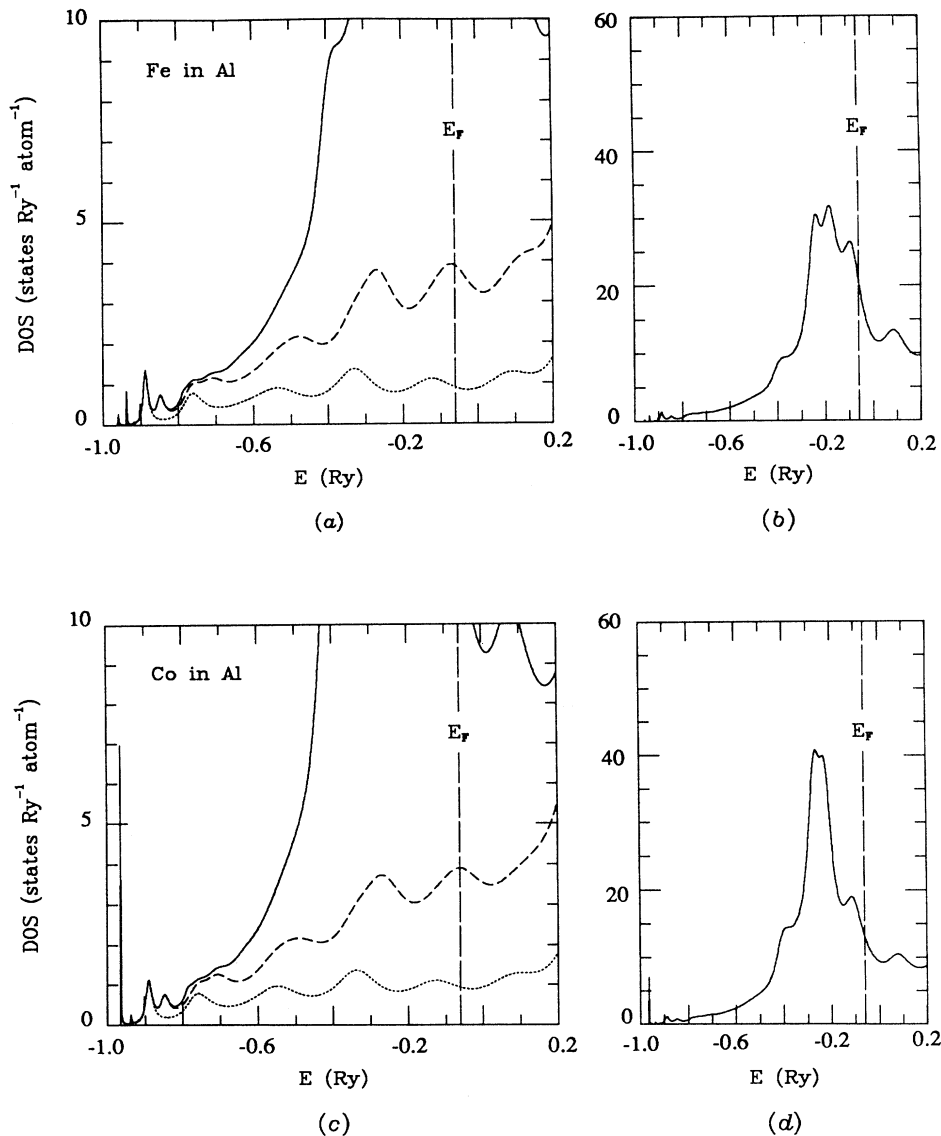


FIG. 5. DOS for Fe in Al (a) and (b) and Co in Al (c) and (d) using the Green's-function recursion method. The key is as in Fig. 3.

function-LMTO) arise due to (i) the use of recursion and (ii) the use of the first-order Hamiltonian  $\mathbf{H}^{(1)}$  in the Green's-function recursion method. The details about the Green's-function-LMTO method can be found in Refs. 5 and 6.

As expected the LDOS calculated with the recursion method is smaller than the LDOS calculated with the Green's-function-LMTO method. According to the recursion calculations,  $AlCr$  has the highest LDOS at  $E_F$  while from the Green's-function-LMTO calculations, we find  $AlMn$  to have the highest LDOS at  $E_F$ . The local densities of states at  $E_F$  for  $3d$  impurities in Al are different from the LDOS in the respective  $3d$  metals. For

example, the LDOS at  $E_F$  for metallic Cr is 9.52 states/Ry while for  $AlCr$  it is 30.02 states/Ry.<sup>30</sup> Similarly, the LDOS at  $E_F$  for  $AlMn$  is higher than the LDOS for metallic Mn. The enhanced LDOS makes the impurity more susceptible to becoming magnetic, which can be seen by considering the Stoner criterion.<sup>14</sup>

In Fig. 7 we compare the LDOS for  $AlTi$  calculated with the Green's-function recursion and the Green's-function-LMTO methods. The differences in the LDOS calculated by the two methods are primarily due to the small size of the cluster and the use of an approximate tight-binding Hamiltonian  $\mathbf{H}^{(1)}$  in the Green's-function recursion method. The use of a small number of exact re-

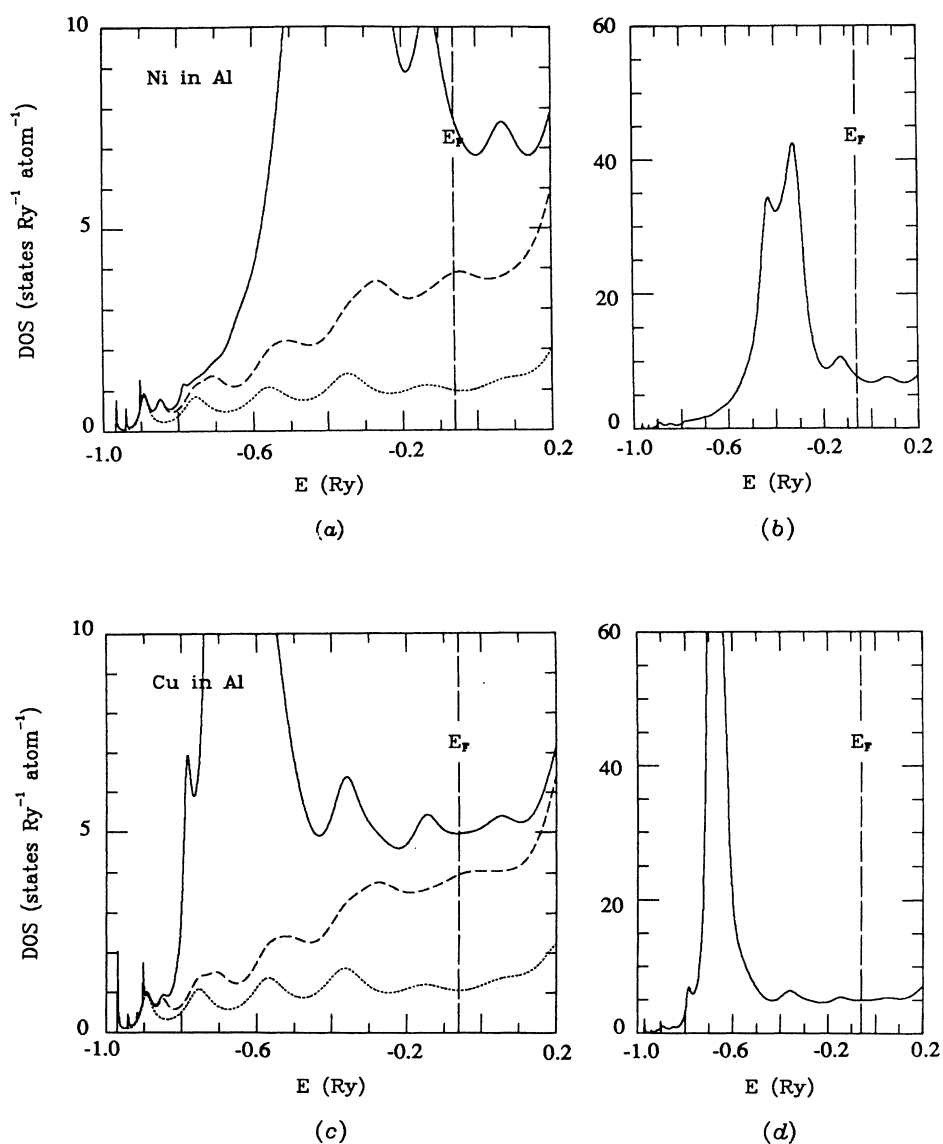


FIG. 6. DOS for Ni in Al (a) and (b) and Cu in Al (c) and (d) using the Green's-function recursion method. The key is as in Fig. 3.



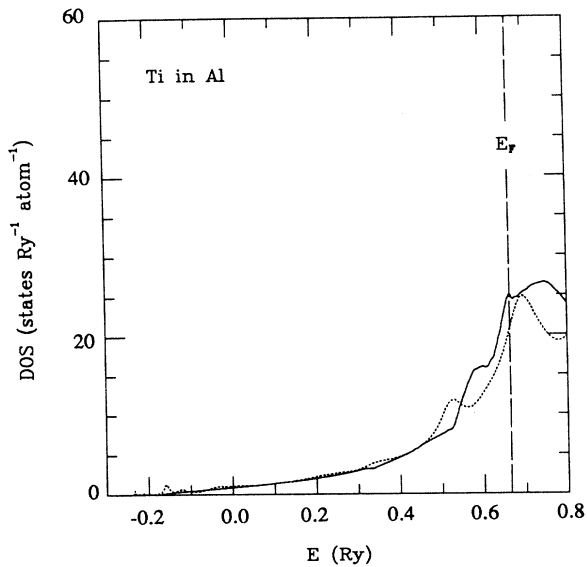


FIG. 7. Comparison of LDOS for Ti in Al calculated with the Green's-function recursion (dotted line) and the Green's-function-LMTO (solid line) methods. Energy scale corresponds to  $V_{MTZ}=0$ .

cursion coefficients, coupled with the Beer and Pettifor termination, introduces some spurious peaks at the edges in the local density of states. These peaks can be clearly seen in the local density of states for  $AlTi$  and  $AlCr$  as well as in  $AlMn$  and  $AlCo$ , as shown in Figs. 4(c) and 5(c), respectively. It is also evident that the first-order Hamiltonian pushes the bottom of the band further down by a few mRy. The bottom of the band can be adjusted by introducing a  $\delta$  function at the impurity site. The impurity local density of states at  $E_F$  for  $AlCr$  calculated with the Green's-function recursion method is small in comparison to the more accurate result of the Green's-function-LMTO method. To improve the recursion results, one must include another energy panel around  $E_F$ . The effect of the combined correction terms in the Green's-function recursion method is not investigated, but its effect in the Green's-function-LMTO method is found to be minimal.<sup>5,6</sup>

## 2. Charge transfer and screening

The impurity atom has a different nuclear charge as well as, in most cases, a different atomic volume from the host atoms surrounding it. These differences force a redistribution of electronic charge around the impurity atom as well as relaxation of the lattice around the impurity. The difference in the local charge on the impurity atom can be partly understood by considering the electronegativity of the impurity and the host atoms, respectively. The use of the host WS radius for describing the impurity cell also affects the amount of charge on the impurity atom. Since we only perturb the impurity site and do not take into account lattice relaxation effects, our calculated charge transfers are uncertain by a small amount. Thus our results cannot be used to predict the direction of charge transfer if the amount of charge transfer is very small.

The amount of charge transfer  $q$  ( $q \equiv N_I - Z$ ) in the impurity WS sphere for 3d impurities in Al is given in Table III. We have also listed the results of Green's-function-LMTO calculations as well as the results of Deutz, Dederichs, and Zeller.<sup>14</sup> According to Green's-function recursion results, all 3d impurities gain some charge from their neighboring Al atoms. Results of Green's-function-LMTO calculations, done with one energy panel, are similar except for  $AlTi$ . For  $AlTi$ , a more accurate calculation done with four energy panels yields  $N_I = 3.48$ , indicating a charge transfer of 0.52 electrons to neighboring Al atoms.<sup>6,14</sup> In the case of a single muffin-tin perturbation, this much local charge is left unaccounted for, but if we were to perturb the nearest neighbors of the impurity atom most of these charge transfers can be included into the self-consistent calculation. For these reasons the amount of charge transfer between impurity and the host atoms cannot be predicted accurately by the calculations done with one perturbed muffin tin. Our results for  $N_I$  are in good agreement with the results of Deutz, Dederichs, and Zeller.<sup>14</sup>

## 3. Virtual bound states

The concept of virtual bound state (VBS) plays an important role in explaining the transport properties of dilute alloys. Almost all the properties of dilute alloys are greatly affected by the associated virtual bound state.

TABLE III. Total LDOS  $n(E_F)$  in states/Ry and the charge transfer  $q$  for 3d transition-metal impurities in Al using the Green's-function recursion method (a), the Green's-function-LMTO method (b), and the calculations of Deutz, Dederichs, and Zeller (c).

Host: Al	a		b		c
Impurity	$n(E_F)$	$q$	$n(E_F)$	$q$	$q$
Ti	22.200	0.018	25.064	-0.012	0.0
V	28.002	0.164	36.138	0.090	0.13
Cr	30.020	0.331	44.168	0.185	0.23
Mn	25.920	0.429	44.714	0.242	0.27
Fe	19.044	0.514	38.724	0.293	0.31
Co	12.400	0.579	26.561	0.326	0.33
Ni	7.532	0.599	12.892	0.333	0.32
Cu	4.978	0.555	4.679	0.277	0.26

Also, the virtual bound states can be directly compared with experiments, and hence provide an important check for the theoretical model. The virtual levels are characterized by high densities of states in the energy spectrum. Thus, whenever Fermi electrons have access to the virtual levels, we expect these levels to have profound effects on the electronic transport and related properties of the dilute alloys.

The movement of the virtual levels in Al can be understood by considering the filling up of the atomic  $d$  level of the impurity atom. For example, let us consider the movement of the virtual levels for  $3d$  impurities in Al. The atomic  $d$  level of Ti with its two  $d$  electrons is well above  $E_F$  of Al. Thus, the corresponding VBS is also well above  $E_F$  but with its position changed due to the interaction with the host atoms. As we add more electrons to the  $d$  orbital and increase the nuclear charge, the atomic  $d$  level lowers its energy, resulting in movement of the VBS towards  $E_F$ . In Figs. 3–6 we see clear evidence of the virtual bound states which are characterized by high densities of states. For example, the VBS for AlV is located around  $E = -0.05$  Ry while for AlNi it is located around  $E = -0.33$  Ry. The virtual bound state crosses  $E_F$  between AlCr and AlMn and it is well inside for AlCu.

## V. SUMMARY AND CONCLUSIONS

We have studied Al-based dilute alloys using the Green's-function recursion method. In this method the impurity atom, taken from  $3d$  series, is surrounded by 488 Al atoms on a fcc lattice. For our self-consistent calculations we have assumed that the impurity potential is localized within the impurity WS sphere. The assumption of only one perturbed muffin tin implies that all the

host atoms, including the nearest-neighbor atoms, are taken to be bulklike. The resulting self-consistent local densities of states at the impurity site give a good description of the changes in the energy spectrum due to the impurity atom.

The Green's-function recursion results for the LDOS and charge transfers are in agreement with the more accurate results of Green's-function-LMTO method, indicating the accuracy of the present approach. The recursion results can be further improved by including (i) the third term,  $\mathbf{h}^\beta \mathbf{o}^\beta \mathbf{h}^\beta$ , in the first-order Hamiltonian given by Eq. (7a), (ii) more than one energy panel, and (iii) the combined correction terms.

Our results are based on perturbing only the impurity muffin tin, but to be able to predict charge transfers between the impurity and the host atoms more accurately, we must perturb at least the nearest-neighbor host atoms. The perturbation of nearest-neighbor atoms can be easily implemented in the Green's-function recursion method but in the Green's-function-LMTO method it leads to a significant increase in the computational effort.

In conclusion, we have presented a first-principles technique, based on local description, for self-consistently calculating the electronic structure of systems without perfect translational symmetry. Its application to Al-based dilute alloys yields results that are in agreement with the results of more accurate methods. The present approach can be readily applied to calculate the electronic structure of surfaces, interfaces, and substitutionally disordered binary alloys.

## ACKNOWLEDGMENTS

Help and guidance of Professor Kian S. Dy during the course of this work is gratefully acknowledged.

- <sup>1</sup>O. K. Andersen and O. Jepsen, *Phys. Rev. Lett.* **53**, 2571 (1984).
- <sup>2</sup>O. K. Andersen, O. Jepsen, and D. Glötzel, in *Highlights of Condensed Matter Theory*, edited by F. Bassani, F. Fumi, and M. P. Tosi (North-Holland, New York, 1985).
- <sup>3</sup>O. K. Andersen, O. Jepsen, and M. Sob, in *Electronic Band Structure and its Applications*, edited by M. Yussouff (Springer-Verlag, Berlin, 1987), p. 1.
- <sup>4</sup>R. Haydock, in *Solid State Physics*, edited by H. Ehrenreich, F. Seitz, and D. Turnbull (Academic, New York, 1980), Vol. 35, p. 215.
- <sup>5</sup>C. Koenig, N. Stefanou, and J. M. Koch, *Phys. Rev. B* **33**, 5307 (1986).
- <sup>6</sup>Prabhakar P. Singh, Ph.D. thesis, University of North Carolina at Chapel Hill, 1989; Prabhakar P. Singh (unpublished).
- <sup>7</sup>J. Friedel, *Can. J. Phys.* **34**, 1190 (1956).
- <sup>8</sup>J. Friedel, *Nuovo Cimento Suppl.* **7**, 287 (1958).
- <sup>9</sup>P. W. Anderson, *Phys. Rev.* **124**, 41 (1961).
- <sup>10</sup>P. A. Wolff, *Phys. Rev.* **124**, 1030 (1960).
- <sup>11</sup>G. Grüner and A. Zawadowski, *Rep. Prog. Phys.* **37**, 1497 (1974); N. Rivier, *J. Phys. F* **4**, L242 (1974); V. Zlatic and N. Rivier, *ibid.* **4**, 732 (1974).
- <sup>12</sup>F. J. Blatt, *Phys. Rev.* **108**, 285 (1957).
- <sup>13</sup>P. Léonard and N. Stefanou, *Philos. Mag. B* **51**, 151 (1985).
- <sup>14</sup>J. Deutz, P. H. Dederichs, and R. Zeller, *J. Phys. F* **11**, 1787 (1981).
- <sup>15</sup>C. Herring, *Phys. Rev.* **57**, 1169 (1940).
- <sup>16</sup>J. M. Ziman, *Principles of the Theory of Solids* (Cambridge University Press, Cambridge, England, 1964).
- <sup>17</sup>W. Kohn and N. Rostoker, *Phys. Rev.* **94**, 1111 (1954); J. Koringa, *Physica* **13**, 392 (1947).
- <sup>18</sup>T. L. Loucks, *Augmented Plane Wave Method* (Benjamin, New York, 1967).
- <sup>19</sup>O. K. Andersen, *Phys. Rev. B* **12**, 3060 (1975).
- <sup>20</sup>H. L. Skriver, *The LMTO Method* (Springer-Verlag, Berlin, 1984).
- <sup>21</sup>R. M. Boulet, J. P. Jan, and H. L. Skriver, *J. Phys. F* **12**, 293 (1982).
- <sup>22</sup>T. Fujiwara and Y. Ishi, in *Microclusters, Proceedings of the First NEC Symposium, Japan, 1986*, edited by S. Sugano, Y. Nishina, and S. Ohnishi (Springer-Verlag, Berlin, 1986), p. 70.
- <sup>23</sup>Prabhakar P. Singh and Kian S. Dy, *Z. Phys. D* (to be published).
- <sup>24</sup>T. Fujiwara, *J. Non-Cryst. Solids* **61-62**, 1039 (1984).
- <sup>25</sup>S. K. Bose, K. Winer, and O. K. Andersen, *Phys. Rev. B* **37**, 6262 (1988).
- <sup>26</sup>P.-O. Löwdin, *Adv. Phys.* **5**, 1 (1956).
- <sup>27</sup>N. Beer and D. Pettifor, in *The Electronic Structure of Com-*

- plex Systems* (NATO Advanced Study Institute, Gent, 1982), edited by N. Temmerman and P. Phariseau (Plenum, New York, 1984).
- <sup>28</sup>*The Recursion Method and its Applications*, edited by D. G. Pettifor and D. L. Weaire (Springer-Verlag, Berlin, 1985).
- <sup>29</sup>U. von Barth and L. Hedin, *J. Phys. C* **5**, 1629 (1972).
- <sup>30</sup>V. L. Moruzzi, J. F. Janak, and A. R. Williams, *Calculated Properties of Metals* (Pergamon, New York, 1978).
- <sup>31</sup>D. A. Papaconstantopoulos, *Handbook of the Band Structure of Elemental Solids* (Plenum, New York, 1986).